Waveguide-fed optical hybrid plasmonic patch nano-antenna

Leila Yousefi and Amy C. Foster *

Department of Electrical and Computer Engineering, Johns Hopkins University, Baltimore, Maryland, USA

** amy.foster@jhu.edu*

Abstract: We propose a novel optical hybrid plasmonic patch nano-antenna for operation at the standard telecommunication wavelength of 1550 nm. The nano-antenna is designed to be compatible with a hybrid plasmonic waveguide through matching of both the operational mode and the wave impedance. The antenna is designed to receive the optical signal from a planar waveguide and redirect the signal out of plane, and is therefore useful for inter- or intra-chip optical communications and sensing. The transmission line model in conjunction with surface plasmon theory is used to develop analytical formulas for design and analysis, and a 3-dimensional full-wave numerical method is used to validate the design. The proposed device provides a bandwidth of more than 15 THz, a gain of 5.6 dB, and an efficiency of 87%. Furthermore, by designing an 8 x 8 array of the proposed antenna, a directivity of 20 dBi and steering of the beam angle are achieved by controlling the relative phase shift between elements of the array.

OCIS codes: (250.5403) Optoelectronics: Plasmonics; (130.3120) Integrated optics: Integrated optics devices.

References and links

1. L. Novotny and N. F. van Hulst, "Antennas for light," Nat Photon **5**, 83–90 (2011).
2. A. G. Curto, G. Volpe, T. H. Taminiau, M. P. Kreuzer, R. Quidant, and N. F. van Hulst, "Unidirectional emission of a quantum dot coupled to a nanoantenna," Science **329**, 930–933 (2010).
3. H. Taminiau, D. Stefani, B. Segerink, and N. F. van Hulst, "Optical antennas direct single-molecule emission," Nat Photon **2**, 234–237 (2008).
4. T. Shegai, S. Chen, V. D. Miljkovic, G. Zengin, P. Johansson, and M. Kall, "A bimetallic nanoantenna for directional colour routing," Nat Commun **2**, 481–486 (2011).
5. T. H. Taminiau, F. D. Stefani, and N. F. van Hulst, "Enhanced directional excitation and emission of single emitters by a nano-optical yagi-uda antenna," Opt. Express **16**, 10858–10866 (2008).
6. N. Yu, P. Genevet, M. A. Kats, F. Aieta, J. P. Tetienne, F. Capasso, and Z. Gaburro, "Light propagation with phase discontinuities: Generalized laws of reflection and refraction," Science **334**, 333–337 (2011).
7. L. Novotny, "Effective wavelength scaling for optical antennas," Phys. Rev. Lett. **98**, 266802 (2007).
8. J. Wessel, "Surface-enhanced optical microscopy," J. Opt. Soc. Am. B **2**, 1538–1541 (1985).
9. U. C. Fischer and D. W. Pohl, "Observation of single-particle plasmons by near-field optical microscopy," Phys. Rev. Lett. **62**, 458–461 (1989).
10. J. Alda, J. M. Rico-Garca, J. M. Lpez-Alonso, and G. Boreman, "Optical antennas for nano-photonic applications," Nanotechnology **16**, S230 (2005).
11. F. Gonzlez and G. Boreman, "Comparison of dipole, bowtie, spiral and log-periodic ir antennas," Infrared Physics & Technology **46**, 418–428 (2005).
12. R. D. Grober, R. J. Schoelkopf, and D. E. Prober, "Optical antenna: Towards a unity efficiency near-field optical probe," Appl. Phys. Lett. **70**, 1354–1356 (1997).
13. J. N. Farahani, D. W. Pohl, H. J. Eisler, and B. Hecht, "Single quantum dot coupled to a scanning optical antenna: A tunable superemitter," Phys. Rev. Lett. **95**, 017402 (2005).

#167929 - $15.00 USD Received 8 May 2012; revised 14 Jul 2012; accepted 18 Jul 2012; published 26 Jul 2012

14. H. G. Frey, S. Witt, K. Felderer, and R. Guckenberger, "High-resolution imaging of single fluorescent molecules with the optical near-field of a metal tip," Phys. Rev. Lett. **93**, 200801 (2004).
15. A. Alu and N. Engheta, "Input impedance, nanocircuit loading, and radiation tuning of optical nanoantennas," Phys. Rev. Lett. **101**, 043901 (2008).
16. A. Alu and N. Engheta, "Hertzian plasmonic nanodimer as an efficient optical nanoantenna," Phys. Rev. B **78**, 195111 (2008).
17. H. J. Lezec, A. Degiron, E. Devaux, R. A. Linke, L. Martin-Moreno, F. J. Garcia-Vidal, and T. W. Ebbesen, "Beaming light from a subwavelength aperture," Science **297**, 820–822 (2002).
18. M. W. Maqsood, R. Mehfuz, and K. J. Chau, "Design and optimization of a high-efficiency nanoscale $\pm$ 90 degree light-bending structure by mode selection and tailoring," Appl. Phys. Lett. **97**, 151111 (2010).
19. S. Sederberg and A. Elezzabi, "Sierpiski fractal plasmonic antenna: a fractal abstraction of the plasmonic bowtie antenna," Opt. Express **19**, 10456–10461 (2011).
20. S. Sederberg and A. Y. Elezzabi, "Nanoscale plasmonic contour bowtie antenna operating in the mid-infrared," Opt. Express **19**, 15532–15537 (2011).
21. L. Tang, S. E. Kocabas, S. Latif, A. K. Okyay, D. Ly-Gagnon, K. C. Saraswat, and D. A. B. Miller, "Nanometre-scale germanium photodetector enhanced by a near-infrared dipole antenna," Nat Photon **2**, 226–229 (2008).
22. L. Cao, J. S. Park, P. Fan, B. Clemens, and M. L. Brongersma, "Resonant germanium nanoantenna photodetectors," Nano Lett. **10**, 1229–1233 (2010).
23. J. N. Anker, W. P. Hall, O. Lyandres, N. C. Shah, J. Zhao, and R. P. Van Duyne, "Biosensing with plasmonic nanosensors," Nat Mater **7**, 442–453 (2008).
24. Y. D. Wilde, F. Formanek, R. Carminati, B. Gralak, P. A. Lemoine, K. Joulain, J. P. Mulet, Y. Chen, and J. J. Greffet, "Thermal radiation scanning tunnelling microscopy," Nature **444**, 740–743 (2006).
25. J. A. Schuller, T. Taubner, and M. L. Brongersma, "Optical antenna thermal emitters," Nat Photon **3**, 658–661 (2009).
26. L. Novotny and S. J. Stranick, "Near-field optical microscopy and spectroscopy with pointed probes," Ann. Rev. Phys. Chem. **57**, 303–331 (2006).
27. R. Salvador, A. Martinez, C. Garcia-Meca, R. Ortuno, and J. Marti, "Analysis of hybrid dielectric plasmonic waveguides," Selected Topics in Quantum Electronics, IEEE Journal **14**, 1496–1501 (2008).
28. I. Avrutsky, R. Soref, and W. Buchwald, "Sub-wavelength plasmonic modes in a conductor-gap-dielectric system with a nanoscale gap," Opt. Express **18**, 348–363 (2010).
29. M. Wu, Z. Han, and V. Van, "Conductor-gap-silicon plasmonic waveguides and passive components at subwavelength scale," Opt. Express **18**, 11728–11736 (2010).
30. R. F. Oulton, V. J. Sorger, T. Zentgraf, R. M. Ma, C. Gladden, L. Dai, G. Bartal, and X. Zhang, "Plasmon lasers at deep subwavelength scale," Nature **461**, 629–632 (2009).
31. R. F. Oulton, V. J. Sorger, D. A. Genov, D. F. P. Pile, and X. Zhang, "A hybrid plasmonic waveguide for subwavelength confinement and long-range propagation," Nat Photon **2**, 496–500 (2008).
32. J. Guo and R. Adato, "Control of 2d plasmon-polariton mode with dielectric nanolayers," Opt. Express **16**, 1232–1237 (2008).
33. K. Wang and A. C. Foster, "Optimization of cmos-compatible hybrid plasmonic waveguides for nonlinear applications," in "OSA Technical Digest (CD)," (Optical Society of America, 2011), JTuB15 (2011).
34. D. Dai and S. He, "A silicon-based hybrid plasmonic waveguide with a metal cap for a nano-scale light confinement," Opt. Express **17**, 16646–16653 (2009).
35. D. Dregely, R. Taubert, J. Dorfmuller, R. Vogelgesang, K. Kern, and H. Giessen, "3d optical yagi-uda nanoantenna array," Nat Commun **2**, 10.1038 (2011).
36. K. J. A. Ooi, P. Bai, M. X. Gu, and L. K. Ang, "Design of a monopole-antenna-based resonant nanocavity for detection of optical power from hybrid plasmonic waveguides," Opt. Express **19**, 17075–17085 (2011).
37. A. Yaacobi, E. Timurdogan, and M. R. Watts, "Vertical emitting aperture nanoantennas," Opt. Letters **37**, 1454–1456 (2012).
38. Q. Song, S. Campione, O. Boyraz, and F. Capolino, "Silicon-based optical leaky wave antenna with narrow beam radiation," Opt. Express **19**, 8735–8749 (2011).
39. R. F. Oulton, "Surface plasmon lasers: sources of nanoscopic light 15," Materials Today **15**, 26–34 (2012).
40. F. Amzajerdian, D. F. Pierrottet, L. B. Petway, G. D. Hines, and V. E. Roback, "Lidar systems for precision navigation and safe landing on planetary bodies," NASA. Technical Reports (2011).
41. C. K. Toth, "R&d of mobile lidar mapping and future trends," in "Proceeding of ASPRS 2009 Annual Conference (Baltimore, Maryland)", (2009).
42. J. M. Pitarke, V. M. Silkin, E. V. Chulkov, and P. M. Echenique, "Theory of surface plasmons and surface-plasmon polaritons," Reports on Progress in Physics **70**, 1–88 (2007).
43. D. M. Pozar, *Microwave Engineering, 2nd Edition* (John Wiley and Sons, 1998).
44. P. B. Johnson and R. W. Christy, "Optical constants of the noble metals," Phys. Rev. B **6**, 4370–4379 (1972).
45. C. A. Balanis, *Antenna Theory: Analysis and Design, 3rd Edition* (Wiley, 2005).
46. J. Pfeifle, L. Alloatti, W. Freude, J. Leuthold, and C. Koos, "Silicon-organic hybrid phase shifter based on a slot waveguide with a liquid crystal cladding," Opt. Express **20**, 15359–15376 (2012).

#167929 - $15.00 USD Received 8 May 2012; revised 14 Jul 2012; accepted 18 Jul 2012; published 26 Jul 2012

1. Introduction

Recently optical nano-antennas have received significant attention due to their ability to control the emission and scattering of light with a nano-scale footprint [1]-[21]. A variety of nano-antennas have been investigated as scatterers to redirect incident light [4, 6], or as devices to control the emission of point sources such as quantum dots [2] and biological emitters [3]. Additionally, nano-antennas have been proposed to enhance the efficiency of photodetection [21, 22], sensing [23], heat transfer [24, 25] and spectroscopy [26].

Previous demonstrations of nano-antennas have primarily focused on controlling the distribution of the local field when dealing with incident light from free-space or a point source [1]-[21]. Such devices have great importance in applications such as sensing [23] and spectroscopy [26]. However, when designing antennas for optical communication purposes, the antenna must be able to receive an optical signal in-plane and radiate it to free space and through reciprocity, must be able to receive the signal from free-space and transmit in-plane. Additionally, the far-field specifications of the antennas must be optimized for angle and maximum directivity.

Here we propose a novel waveguide-fed hybrid plasmonic patch nano-antenna to operate at the standard telecommunication wavelength of 1550 nm. The antenna has been impedance-matched with the characteristic impedance of the hybrid plasmonic waveguide feed. Therefore, the antenna can receive the optical signal from the hybrid plasmonic waveguide feed (free-space) efficiently, and direct it to free space (the hybrid plasmonic waveguide feed). The nano-antenna and hybrid plasmonic waveguide feed can be fabricated utilizing standard CMOS processing techniques, and therefore can be integrated with other elements in an opto-electronic circuit. Additionally we show that a highly directive pattern of 20 dBi can be achieved by using an 8 x 8 array of patch antennas. Furthermore, we numerically demonstrate beam steering through controlling the phase shift between elements in the antenna array.

Previous studies have shown that a hybrid plasmonic waveguide supports a hybrid plasmonic quasi-transverse magnetic (TM) mode in which the field is primarily confined inside the lower index material resulting in low loss waveguiding structures [27]-[34]. Here we exploit the sub-wavelength mode confinement and low loss properties of hybrid plasmonic structures to develop a highly efficient and directive patch nano-antenna. The proposed nano-antenna has a higher efficiency than plasmonic antennas [35]-[37], while simultaneously having a smaller footprint than dielectric antennas [38].

The proposed nano-antenna is useful for several applications. In particular, inter and intra-chip optical communications can utilize two antennas as a transmitter and receiver to provide a wireless optical link between optical circuits on different layers and/or different chips. This application will be especially useful to couple the optical energy from integrated lasers [39] to various layers of an optical circuit. Another potential application is in LIDAR mapping systems [40, 41], where an array of the proposed antenna can be used to perform beam-steering for detection and tracking of moving targets.

2. Analytical Approach

The nano-antenna and waveguide feed (as shown in Fig. 1) have been designed based on the hybrid plasmonic structure [27]-[34], where a very thin layer of a low refractive index material (SiO_2) is sandwiched between a higher refractive index material (Si) and a metal (Ag).

In order to avoid reflection, the antenna is designed to have an input impedance equal to the wave impedance of the hybrid plasmonic feeding waveguide. Here, we use surface plasmon theory [42] in conjunction with the transmission line model [43] to develop analytical formulas to determine the input impedance of the patch antenna and the wave impedance of the plasmonic waveguide.

The transmission line model can be used only for fields in TEM modes, where both electric

#167929 - $15.00 USD Received 8 May 2012; revised 14 Jul 2012; accepted 18 Jul 2012; published 26 Jul 2012

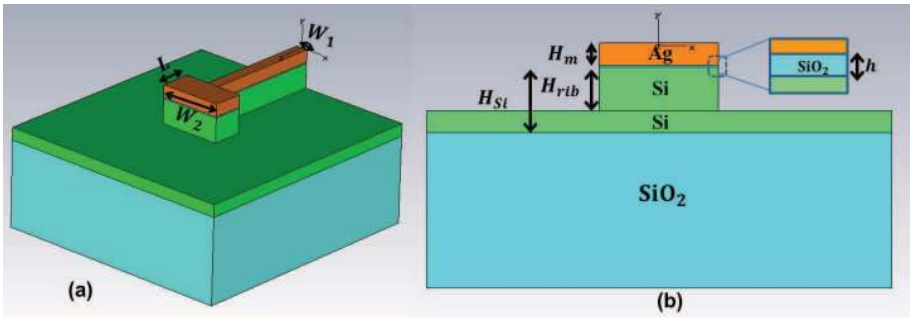

Fig. 1. Patch nano-antenna fed by a plasmonic hybrid waveguide (a) Perspective view (b) Cross-sectional schematic.

and magnetic field have no component in the propagation direction (the z direction in Fig. 1). According to surface plasmon theory, the hybrid plasmonic mode supported by the structure shown in Fig. 1 is a TM mode with electric field both in the y and z directions [42]. However, here we show that the z-component of the electric field is much smaller than the y-component, and therefore, the resultant hybrid plasmonic TM mode can be approximated as a TEM mode. According to surface plasmon theory [42], the ratio of the y-component to the z-component of the E-field is equal to:

$$\frac{E_y}{E_z} = \frac{K_z}{K_y} = \frac{\frac{\omega}{c}\sqrt{\frac{\varepsilon_m \varepsilon_d}{\varepsilon_m + \varepsilon_d}}}{\frac{\omega}{c}\sqrt{\frac{\varepsilon_d^2}{\varepsilon_m + \varepsilon_d}}} = \sqrt{\frac{\varepsilon_m}{\varepsilon_d}} \tag{1}$$

where K_y and K_z are propagation constants in the y and z directions, respectively, ω is the radial frequency, c is the propagation velocity of the light in the vacuum, ε_d is the permittivity of the dielectric (SiO_2 in this design), and ε_m is the permittivity of the metal (Ag in this design).

Since at optical frequencies metals have a negative permittivity whose magnitude is much larger than that of dielectrics, $|\varepsilon_m| \gg \varepsilon_d$, the y-component of the electric field will be much larger than the z-component. Therefore the z-component is negligible and use of the transmission line model is valid. In this design, the permittivity of silver at the wavelength of 1550 nm is assumed to be $\varepsilon_{Ag} = -129 + j3.28$; a value extracted from fitting the experimental data from [44] with a Drude function (due to the fact that data in [44] is limited to a few wavelengths, fitting is necessary to provide the dielectric constant at all desired wavelengths). Considering the value of the dielectric constant of SiO_2 as $\varepsilon_{SiO_2} = n_{SiO_2}^2 = 2.09$, the ratio in (1) will be equal to $0.1 + j7.85$. In other words, for our design the magnitude of the y-component of the electric field is predicted to be 7.85 times higher than the magnitude of the z-component, therefore for design purposes the behavior of our device can be accurately predicted with the transmission line model.

Using the transmission line model at the resonance frequency, the input impedance of the patch antenna when fed from the side is calculated as [45]:

$$Z_{antenna} = \frac{1}{Y_{in}} = \frac{1}{2G}, \quad G = \frac{W_2}{120\lambda_0}[1 - \frac{1}{24}(\frac{2\pi h}{\lambda_0})^2] \tag{2}$$

where W_2 is the width of the patch antenna and h is the height of SiO_2 layer (see Fig. 1). The characteristic impedance of the plasmonic feeding waveguide is calculated as [43]:

$$Z_{Waveguide} = \frac{Z_0}{n_{eff}} = \frac{377}{n_{eff}} \tag{3}$$

#167929 - $15.00 USD Received 8 May 2012; revised 14 Jul 2012; accepted 18 Jul 2012; published 26 Jul 2012

where Z_0 is the characteristic impedance of air, and n_{eff} is the effective refractive index of the plasmonic mode.

As shown in previous demonstrations of the plasmonic hybrid waveguide, the effective refractive index is non-linearly dependent on the width of the metal, W, and height of the SiO_2 layer, h [27]-[34]. To derive a formula that relates the refractive index, n_{eff} to the parameters W and h, we numerically calculate the real component of n_{eff} for different values of W and h using the Computer Simulation Technology (CST) software and then apply curve fitting. Figure 2 illustrates the numerically calculated real component of n_{eff} for different values of W and h and the resulting relationship is shown in (4). In equation (4), W and h are in μm.

In this fitting process, the other parameters include a free space wavelength of $\lambda_0 = 1550\ nm$, effective permittivity of silver $\varepsilon_{Ag} = -129 + j3.28$, and the three heights (see Fig. 1(b)) are $H_m = 100\ nm$, $H_{rib} = 200\ nm$ *and* $H_{Si} = 300\ nm$.

$$n_{eff} = \sqrt{\frac{\varepsilon_d \varepsilon_m}{\varepsilon_d + \varepsilon_m}} F(W,h), \quad F(W,h) = \frac{1 + 1798W + 3114h + 10.55Wh}{32300 + 759.7W + 3337h + 10.55Wh} \tag{4}$$

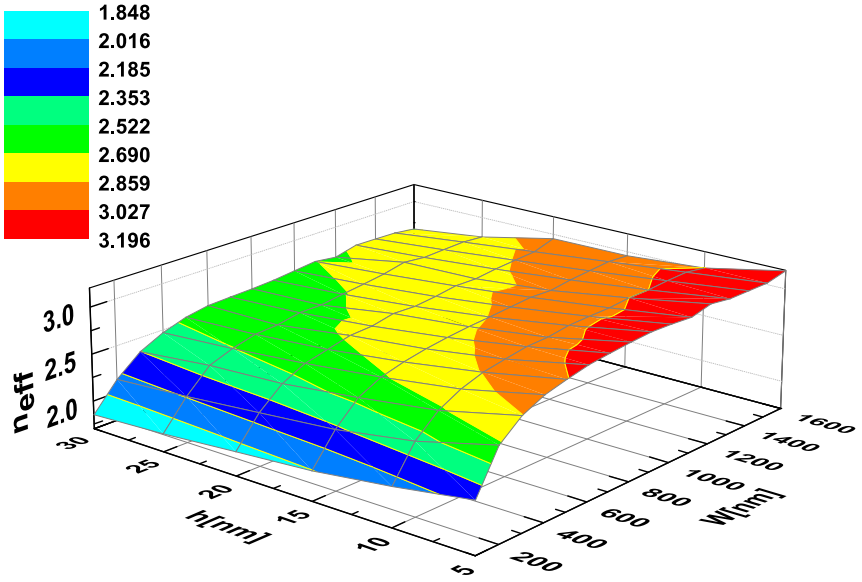

Fig. 2. Numerically calculated real component of the effective refractive index, n_{eff}.

Using (2)-(4), and fixing the height of the SiO_2 layer as $h = 10\ nm$, the width of the waveguide and the antenna are calculated as $W_1 = 100\ nm$, and $W_2 = 520\ nm$, respectively, providing a perfect impedance match between the antenna and the waveguide.

The resonance frequency of the antenna as determined by the resonance length, L, is equal to half of the free space wavelength (1550 nm in this design) divided by the effective refractive index, n_{eff}. Using the values of $W_2 = 520\ nm$, and $h = 10\ nm$, the real component of the effective refractive index of our structure as determined by (4) is $n_{eff} = 2.88$, resulting in a resonance length of $L = 270\ nm$.

#167929 - $15.00 USD Received 8 May 2012; revised 14 Jul 2012; accepted 18 Jul 2012; published 26 Jul 2012

It should be noted that the matching has been achieved for only the real component of the impedances. At the resonance frequency (where the length of patch antenna is equal to half of the wavelength) the imaginary component of the input impedance of the patch antenna would be zero. However, due to the plasmonic losses, the characteristic impedance of the plasmonic waveguide will have both real and imaginary components. The imaginary part, although much smaller than the real part, is non-negligible due to the loss of plasmonic mode, resulting in a partial reflection of of the wave. However, since the imaginary component is much smaller than the real component, the reflected wave is expected to be minimal.

3. Numerical Analysis

To verify the analytical approach developed in Section 2, we numerically simulate our waveguide-fed optical hybrid plasmonic patch nano-antenna for operation at the telecommunication wavelength of 1550 nm. In this simulation, 3-dimensional full-wave numerical analysis is carried out using frequency domain analysis in CST microwave studio. Figure 3 shows the magnitude of the dominant component of the electrical field, E_y at the cross section of the hybrid plasmonic waveguide that feeds the nano-antenna. As shown in this figure, the field is primarily confined in the 10 nm SiO_2 layer, confirming the excitation of the hybrid plasmonic TM mode. These results are achieved using the port solver in CST microwave studio.

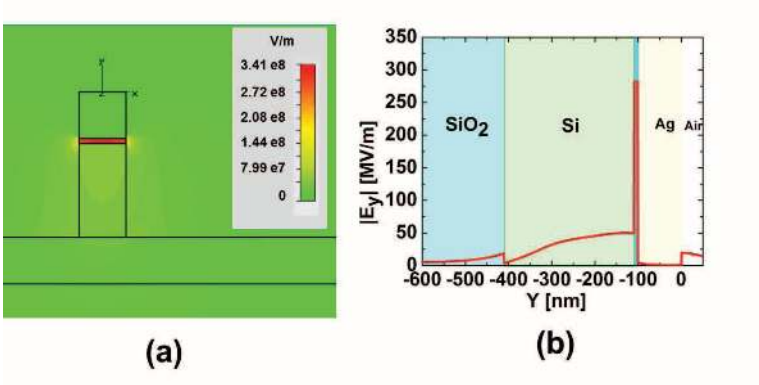

Fig. 3. Numerically calculated y-component of electric field, $|E_y|$ (a) in two dimensions at the cross section of the hybrid plasmonic waveguide that feeds the nano-antenna and (b) in one dimension when x = 0.

Figure 4 compares the values of the different components of the electric field in the waveguide and in the antenna. In this figure, the magnitude of the electric field is reported at the center of the SiO_2 layer as a function of z (when x = 0 and y = -105 nm). As shown in Fig. 4, the y-component is more than an order of magnitude larger than the z-component, and the field can therefore be approximated as a TEM mode as predicted by analytical formulas explained in Section 2. These results further validate the use of the transmission line model for design and analysis of both the hybrid plasmonic feeding waveguide and the patch nano-antenna in the analytical approach.

Figure 5 illustrates the ratio of the reflected wave to the incident wave, S_{11}, as a function of the operation frequency for our waveguide-fed optical nanoantenna. The results are achieved from full-wave numerical analysis in CST. In this analysis, the frequency-dependent property of the permittivity of the silver, ε_{Ag}, is also included using the dependence from [44]. The resultant S_{11} of our waveguide-fed optical nanoantenna is better than -10 dB at the resonance frequency of 193.5 THz (1550 nm), verifying the impedance matching between the waveguide and the

#167929 - $15.00 USD Received 8 May 2012; revised 14 Jul 2012; accepted 18 Jul 2012; published 26 Jul 2012

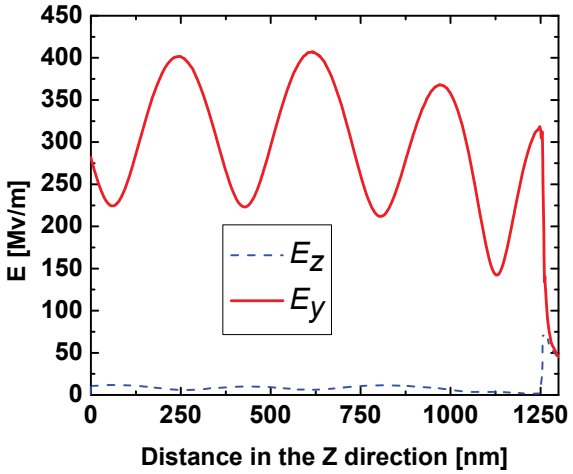

Fig. 4. The magnitude of the different components of the electric field at the center of the SiO_2 layer (x = 0 and y = -105 nm) for different values of z, and at the wavelength of 1550 nm.

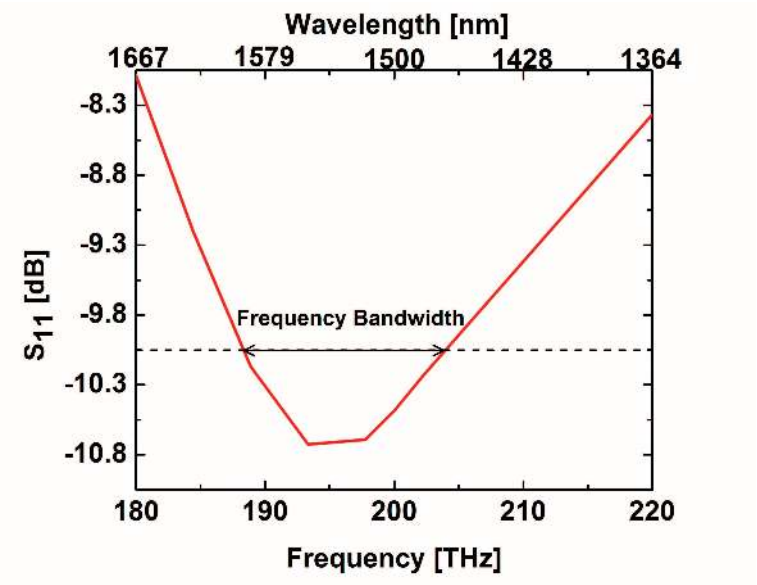

Fig. 5. Numerically calculated ratio of the reflected wave to the incident wave, S_{11}, versus operation frequency and wavelength.

antenna. The frequency bandwidth of the antenna where $S_{11} < -10\ dB$ is 15.6 THz, or 8%. This bandwidth corresponds to the wavelength range of 1463 nm-1580 nm, which covers most of the standard optical communication bands of S and C.

The radiation pattern of the waveguide-fed optical nanoantenna is shown in Fig. 6, illustrating the out-of-plane directivity for inter- and intra-chip communications, and a maximum gain of 5.64 dB; a value competitive with standard microwave-based patch antennas. The total efficiency of the antenna, defined as the ratio of the radiated power over the total power entering

#167929 - $15.00 USD Received 8 May 2012; revised 14 Jul 2012; accepted 18 Jul 2012; published 26 Jul 2012

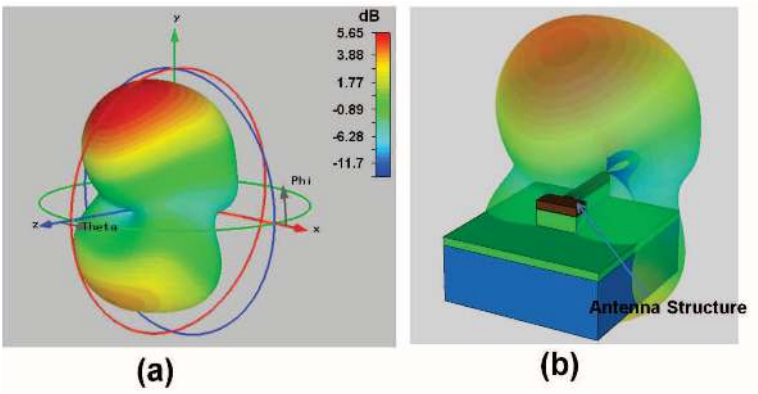

Fig. 6. 3-D Radiation gain plot, (a) Radiation pattern alone (b) Radiation pattern with the nano-antenna structure superimposed for reference.

the waveguide, is numerically calculated as 87%. Unlike typical microwave patch antennas, our nano-antenna is designed without a ground plane providing a radiation pattern that is shifted slightly off-axis (y-axis in Fig. 1), with the maximum of the upward and downward radiations to occur at 30 and 35 degrees from the y-axis, respectively. The absence of the ground plane is essential to provide the bidirectional (+y and -y) radiation pattern allowing for communication functionality in sophisticated multi-layer optical circuits.

4. Antenna Array and Potential Beam-Steering Applications

Here we numerically investigate the performance of the designed patch antenna when used in an antenna array. Figure 7 illustrates the resultant radiation pattern of an 8 x 8 array of the designed patch antenna when the feeding signal has the same phase for all the antenna elements in the array. The periodicity of the antenna elements in the array is 800 nm. As shown in Fig.7, a significantly improved directivity of 21.8 dBi can be achieved with this array, which only occupies a 5.6 μm by 5.6 μm footprint.

The results shown in Fig. 7 are achieved using the array-toolkit in the CST simulation software, which uses the array factor formula [45] to calculate the array pattern from a single element pattern. In this calculation, the coupling between the antenna elements is ignored, however given that the distance between the antennas in this design is greater than 280 nm (more than half of the effective wavelength of the hybrid plasmonic mode), and that the field is highly confined in the SiO_2 layer, the coupling between the antennas is assumed to be minimal, and therefore has a negligible effect on the resultant radiation pattern. However, further investigation on optimizing the coupling effect will be considered in future work.

Beam steering can be achieved in the antenna array by controlling the relative phase between the antenna elements. Figure 8 demonstrates how the pattern evolves when the phase shift between the antenna elements varies from $\Delta\phi = -90^\circ$ to $\Delta\phi = +90^\circ$. As shown in this figure, the direction of the pattern can be steered by controlling the relative phase shift between the planar optical signals in each feeding waveguide. This could be achieved, for example, by integrating highly efficient active phase shifters [46] into each arm of the antenna array. Such phase shifters can achieve 180° phase shift with less than 1 V of applied bias, and therefore proper power budgeting can be performed for the appropriate application. The beam steering capability is especially useful when the antenna is used in the receiving mode, and the direction of the receiving optical beam varies. For example, this capability is very useful in LIDAR systems when detecting and tracking moving targets [40, 41]. Another interesting application

#167929 - $15.00 USD Received 8 May 2012; revised 14 Jul 2012; accepted 18 Jul 2012; published 26 Jul 2012

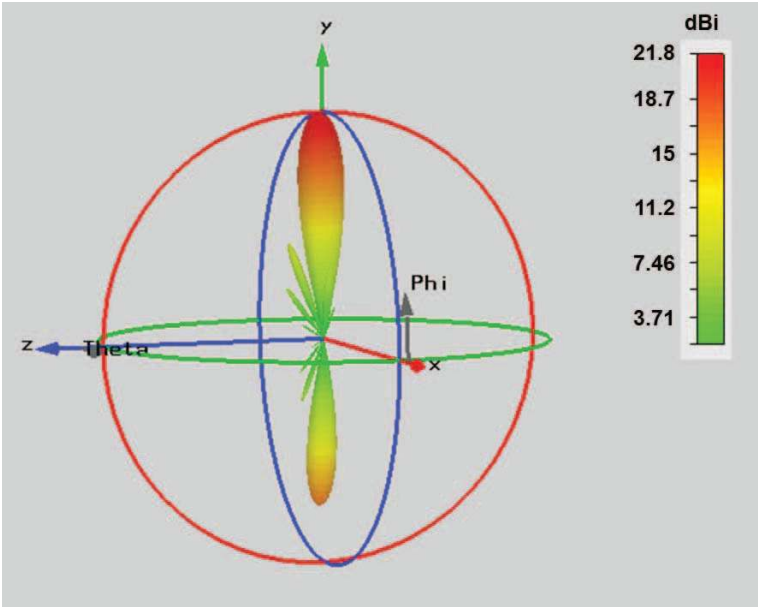

Fig. 7. 3-D Radiation pattern of a 8x8 array of the designed patch antenna.

of the beam-steering capability is in developing efficient solar cells, when optical antennas are used to receive the solar energy from the sun. In this application, the array antenna with beam-steering capability could potentially track the sun during the day to ensure maximum energy conversion.

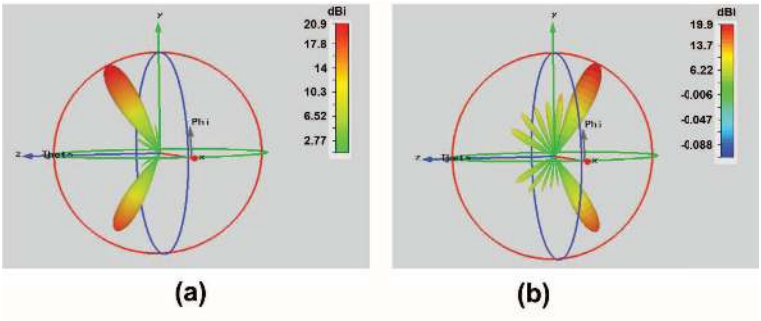

Fig. 8. Using the designed antenna for beam-steering applications (a) The resultant pattern when $\Delta\phi = -90^\circ$, (b) The resultant pattern when $\Delta\phi = +90^\circ$.

5. Conclusion

A novel plasmonic optical patch nano-antenna is designed to be matched to and therefore fed by a hybrid plasmonic waveguide. Surface plasmon theory and the transmission line model are used to develop an analytical formula for the calculation of impedances of the antenna and the plasmonic waveguide feed. The developed formulas are utilized to design a nano-antenna that operates at the standard telecommunication wavelength of 1550 nm. The radiation pattern of the analytically-designed antenna is numerically simulated using CST microwave studio,

#167929 - $15.00 USD Received 8 May 2012; revised 14 Jul 2012; accepted 18 Jul 2012; published 26 Jul 2012

demonstrating a broad bandwidth greater than 15 THz, a large gain of 5.64 dB, and an efficiency of 87%. The waveguide-fed plasmonic patch antenna can be fabricated using standard CMOS processing, providing not only a means for communication between multiple optical devices layers, but also holding potential for highly-integrated optical beam-steering devices such as active LIDAR target tracking and improved solar cell efficiency through solar tracking.

6. Acknowledgements

This work was supported by start-up funds from the Johns Hopkins University.

#167929 - $15.00 USD Received 8 May 2012; revised 14 Jul 2012; accepted 18 Jul 2012; published 26 Jul 2012